The mammalian auditory hair cell: A simple electric circuit model

F. Rattay and I. C. Gebeshuber
University of Technology, Vienna, Austria

A. H. Gitter
Institut für klinische Physiologie, Freie Universität, Berlin, Germany

(Received 5 February 1997; revised 1 November 1997; accepted 2 November 1997)

A model based on the potassium current pathway through the hair cell is used to analyze the electrical behavior of mammalian inner and outer hair cells. Without taking into account the effects of calcium it is possible to simulate experimental results concerning the shape and strength of the receptor potential and the frequency dependent ac (alternating current) and dc (direct current) components of the receptor current. This model and a simplified form of it are utilized to explain: (1) Transduction latencies: that the receptor potential follows a stimulating signal with a very short delay, under the assumption of a constant number of open K^+ channels in the lateral part of the cell membrane. (2) Transduction gains: why higher potential changes are measured in inner hair cells than in outer hair cells, although the outer hair cells are expected to be exposed to higher stereociliary motions: in inner hair cells a decrease in the conductance of the basolateral membrane causes higher gain (receptor potential increases) and together with an increase of membrane capacitance slower reaction (a larger time constant). (3) Transduction channel kinetics: that the shortest (0.1 ms) as well as the longest (20 ms) possible open times of the transduction channels in the stereocilia have different frequency related effects on the shape of the receptor potentials.
© *1998 Acoustical Society of America.* [S0001-4966(98)03503-6]

PACS numbers: 43.64.Ld, 43.64.Bt, 43.64.Nf [RDF]

INTRODUCTION

In vertebrates, hair cells are found in all peripheral structures used in hearing and balance. They play the key role in the mechano-electrical transduction mechanism. Inner hair cells (IHC) and outer hair cells (OHC) are found in the mammalian cochlea. Figure 1 schematically illustrates a typical inner hair cell. The apical part of the cell including the hairs (stereocilia) enters the endolymphatic fluid, which is characterized by its high electrical potential and its high K^+ concentration. The stereocilia of one hair cell are connected through tip links and lateral links. The transmembrane voltage of -70 mV for OHC and -40 mV for IHC is mainly caused by the K^+ concentration gradient between cell body and cortilymph. Current influx that changes the receptor potential occurs mainly through the transduction channels of the stereocilia: stereociliary displacement to the lateral side of the cochlea causes an increase of transduction channel open probability and hence depolarization of the receptor potential, whereas stereociliary displacement to the medial side results in a decrease of the transduction channel open probability and hence hyperpolarization. The transduction channel is cation selective and although Ca^{++} ions are important in regulating the opening mechanism of the transduction channels our electric model considers the main current component, carried by K^+ ions entering the cell.

The relation between hair deflection and receptor potential change is asymmetric and saturates (Hudspeth and Corey, 1977; Markin *et al.*, 1993). Small variations of the receptor potential (about 0.1 mV) cause a release of at least one quantum of neurotransmitter which may cause spiking in the most sensitive fibers of the auditory nerve (Hudspeth, 1989). In this respect the effectiveness of synaptic transmission from the hair cell to the auditory nerve fiber is extraordinary compared to common synaptic transmission, e.g., Katz and Miledi (1967) report that there is a threshold for neurotransmitter release at about 45 mV depolarization in the presynaptic terminal of the squid stellate ganglion.

Several hypotheses are concerned with the opening mechanism of the transduction channels in the stereocilia. The most prominent is the gating-spring theory from Hudspeth which proposes that the tip links which connect neighboring stereocilia are elastic elements, called gating springs, that directly open the transduction channels (Pickles *et al.*, 1984). Even the assumption that the gating springs are localized in the horizontal links would not influence the functionality of the transduction mechanism (Gitter, 1994, 1996). Because of the lack of experimental data, our model does not suggest a detailed transduction mechanism process.

Mammalian hair cells are very sensitive and because of their short latency in generating the receptor potential a second messenger system is highly unlikely to be involved. In the present paper we show that a model of the hair cell that just takes into account its electrical properties yields results comparable to those from experiments.

I. ELECTRICAL MODEL OF A HAIR CELL

The main task of hair cells in sensory systems is to detect forces which deflect their stereocilia. Differences in the hair cells of the cochlea and of the vestibular organ appear in ion concentrations, in geometries and membrane

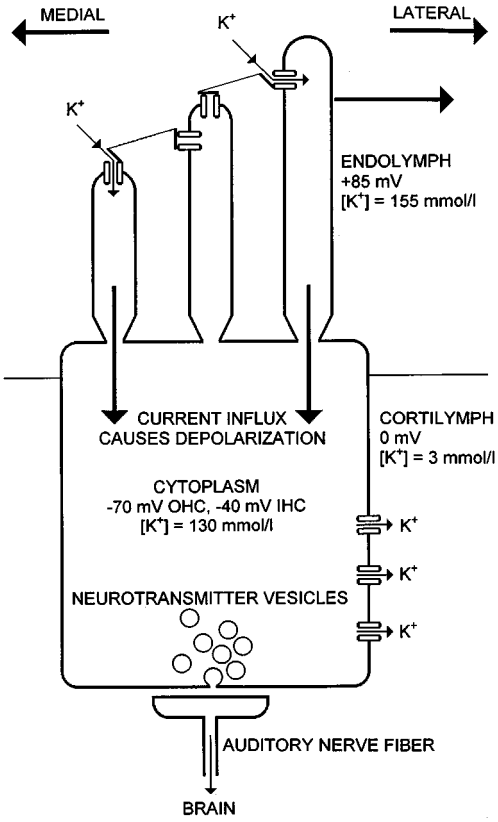

FIG. 1. Scheme of a mammalian cochlear inner hair cell. Experimental results indicate that there are only one or two transduction channels close to the tip of each stereocilium. K^+ influx through open transduction channels causes depolarization inside the hair cell, repolarization occurs then because of K^+ outflux through the lateral cell body membrane.

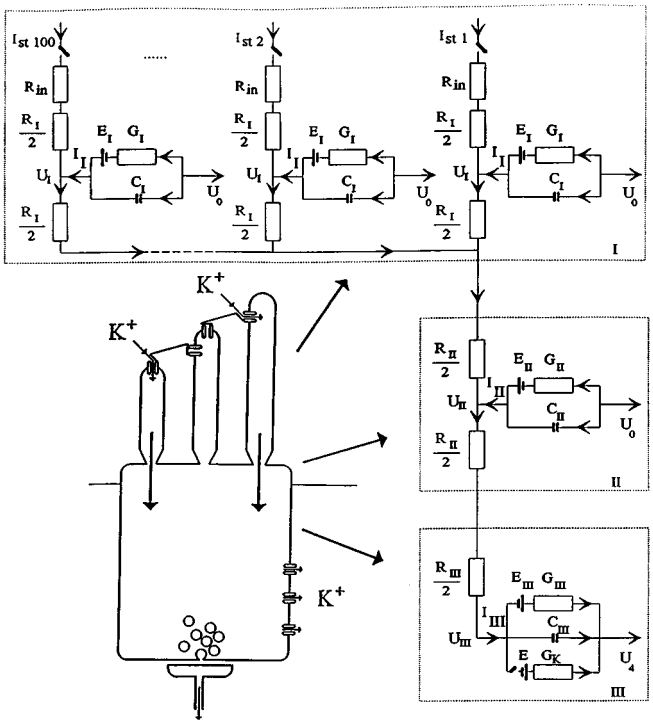

FIG. 2. Equivalent electric circuit diagram of the hair cell's three main regions in our model. Each of the compartments is represented by its mean inside potential U, membrane conductance G, membrane capacitance C, Nernst potential E and cytoplasm resistance R. The K^+ influx through the jth stereociliary transduction channel is represented by the stimulating current I_{stj}. G_K represents the conductance of a K^+ channel in the basolateral cell membrane. U_0 and U_4, the potentials in the endolymph and cortilymph are constant, whereas the potentials in the different hair cell regions, U_I, U_{II} and the receptor potential U_{III}, depend upon stereociliary movement. Note that the values of G_I and C_I depend on the individual stereocilia lengths.

properties. Even in the same cochlea there are remarkable differences between receptor potentials from inner hair cells and outer hair cells (comp. inset of Fig. 3). Konishi and Salt (1983) measured the K^+ activities in the mammalian cochlea at $[K^+]_{\text{endolymph}} = 113.8$ mM, $[K^+]_{\text{cortilymph}} = 1.98$ mM and $[K^+]_{\text{hair cell}} = 64.8$ mM. In our model we used data from Zenner (1994) as shown in Fig. 1 (see also Ma *et al.*, 1996). In the cochlea, the electrical potential of endolymph and cortilymph are 84.7 mV (Konishi and Salt, 1983) and 0 mV (Dallos *et al.*, 1982), respectively. According to Russell and Sellick (1978) and Cody and Russell (1987), the resting potential of cochlear IHC is about -40 mV. The resting potential of OHC is about -70 mV (Dallos *et al.*, 1982).

Our equivalent electric circuit model of a hair cell consists of three different compartments (Fig. 2). The part of the cell body which is surrounded by cortilymph forms compartment III. U_{III} represents the voltage in the center of this compartment, i.e., U_{III} equals the receptor potential. So, when no stimulus is applied U_{III} equals the resting potential. The transition between the cell body and the stereocilia is modeled by compartment II, a spherical part with center voltage U_{II}, whose membrane is surrounded by endolymph-like compartment I, the stereocilia. The current flux through the transduction channels into the stereocilia is modeled individually by subcompartments containing switches, which simulate the opening/closing kinetics of the transduction channels. The single channel transduction current is calculated using the cortilymph-cytoplasm potential difference with constant single channel conductance resulting in 10 and 12 pA for IHC and OHC, respectively. However, our model does not suggest a detailed mechanism for the transduction process since further experimental evidence on the molecular movement associated with transduction is necessary, and the single channel transduction current in our model was assumed to be constant (according to Crawford *et al.*, 1991, the fluctuations in receptor potential do not significantly influence the total charge movement while the transduction channels are open). The open probability of transduction channels depends in a non-linear way on the deflection of the stereocilia; we used the data from Markin *et al.* (1993) for modeling. U_I represents the voltage in the center of each of the stereocilia. On IHC the stereocilia are arranged in three parallel rows, on OHC the three rows of stereocilia are parallel and additionally arranged in W shape. Zetes (1995) reports in IHC stereocilia lengths of 2.024 ± 1.411 μm, and in OHC of 2.070 ± 1.184 μm. In our model we have investigated the influence of stereocilia lengths on the receptor potential changes. We have averaged the stereocilia lengths reported in Zetes (1995), such that the stereocilia bundle is composed of three rows of stereocilia of increasing heights, with equal heights in each row and we have also calculated the influence of uniform stereocilia lengths across the hair bundle.

Each compartment consists of capacity, resistance and

TABLE I. Parameters used for modeling cochlear hair cells.

Parameter	IHC	OHC
number of stereocilia (human, Zenner, 1994)	$n=60$	$n=100$
average length of stereocilia (guinea pig, Zetes, 1995; humans: Zenner, 1994)	$l_I=2$ μm	$l_I=2$ μm
average diameter of stereocilia (guinea pig, Zetes, 1995; Zenner, 1994)	$d_I=0.2$ μm	$d_I=0.2$ μm
length of cell body (Zenner, 1994)	$l_{III}=20$ μm	$l_{III}=50$ μm
diameter of cell body (guinea pig, Preyer *et al.*, 1994)	$d_{III}=8$ μm	$d_{III}=10$ μm
cell body area involved (calculated)	$a_{III}=552$ μm^2	$a_{III}=1649$ μm^2
open probability of transduction channels at rest (bullfrog, Hudspeth, 1989)	0.15	0.15
single transduction channel current (guinea pig, lateral OHC K^+ channel, Gitter *et al.*, 1992)	$I_{tc}=10$ pA	$I_{tc}=12$ pA
input resistance of transduction channel	$R_{in}=0$ Ω	$R_{in}=0$ Ω
cytoplasm resistance (Rattay, 1990)	$\rho_i=100$ Ω cm	$\rho_i=100$ Ω cm
membrane resistance (Rattay, 1990)	$\rho_m=5$ kΩ cm^2	$\rho_m=5$ kΩ cm^2
membrane capacitance (Rattay, 1990; see text)	$c=2$ μF/cm^2	$c=1$ μF/cm^2
cortilymph potential (Zenner, 1994)	$U_4=0$ V	$U_4=0$ V
endolymph potential (Zenner, 1994)	$U_0=85$ mV	$U_0=85$ mV
Nernst potential endolymph-cytoplasm (calculated)	$E_I=E_{II}=4$ mV	$E_I=E_{II}=4$ mV
Nernst potential cytoplasm-cortilymph (calculated)	$E_{III}=43$ mV	$E_{III}=71$ mV
number of K^+ channels in the lateral cell membrane (always open; fitted)	$Kch=260$	$Kch=900$
conductance of a lateral K^+ channel (guinea pig, Gitter *et al.*, 1992)	$G_K=200$ pS	$G_K=200$ pS
cytoplasm resting potential (Russell and Sellick, 1978 and Cody and Russell, 1987; Dallos *et al.*, 1982)	-39.7 mV	-69.9 mV

battery to model the various currents through the membrane. Battery potentials were calculated using data of Zenner (1994). The compartments are connected by resistances, which represent the electrical properties of the cytoplasm. The currents from the open transduction channels combine to a current which flows through compartment II. This current then leads to a receptor potential change in compartment III and leaves the receptor cell through K^+ channels in the basolateral membrane. In the resting state, e.g. when the stereocilia are not deflected, about 15% of the transduction channels are open (Hudspeth, 1989).

There are few data available on the kinetics of transduction channels. Crawford *et al.* (1991) report for a 150-nm displacement of the stereocilia a mean open time of 1.1 ms and a distribution that could be well fitted by a single exponential. Because of this we modeled the open/close kinetics by a Markovian process without memory. The shortest possible transduction channel open time was assumed to be 0.1 ms, the longest 20 ms, as reported for K^+ channels in the lateral cell body membrane of guinea pig outer hair cells (Zenner, 1994).

This model can be used for all kinds of hair cells. Parameters for typical mammalian IHC and OHC which we have used for our calculations are given in Table I. We used an average number of 60 stereocilia for IHC and 100 for OHC, respectively. Note that this does not generally hold in mammalian cochleas, e.g., in the apex of the guinea pig cochlea OHC in the second and third rows frequently have less than three rows of stereocilia. IHC cell body lengths show small variations within a single cochlea, OHC cell body lengths, however, vary, at the apex of the cochlea they can be three times as long as they are at the base (Spoendlin, 1970). We modeled IHC with a length of 20 μm and OHC with an average length of 50 μm, according to Zenner (1994).

Our results show that for the prediction of the receptor potential in compartment III, the compartments I and II can be omitted because the leakage through the membranes of these two compartments is very small.

II. RESULTS

There are differences in the time constants and amplitudes of receptor potential reactions of inner and outer hair cells to a stimulus of 1 ms duration, which is strong enough to open all of the transduction channels (Fig. 3). Here we assume that 15% of the transduction channels are always open, and the rest switches from closed to open state while the stimulus pulse is applied. The main differences between IHC and OHC in physiological parameters are (see also Table I): Compared to an OHC an IHC has fewer stereocilia with a larger variance in lengths, a smaller cell body, a higher membrane capacitancy, and fewer K^+ channels because of the smaller basolateral membrane area involved (leading to a smaller resting potential). In our view OHC are also expected to be exposed to higher stereociliary motions because of their localization close to the mainly moving parts of the basilar membrane. The inset of Fig. 3 shows the relating experimental data from Dallos (1983).

A. Transduction latencies

Modeling an OHC without any open lateral K^+ channels results in a time constant of the receptor potential change of 5 ms, because only current outflux via the membrane is possible in this situation. The IHC capacitance is modeled

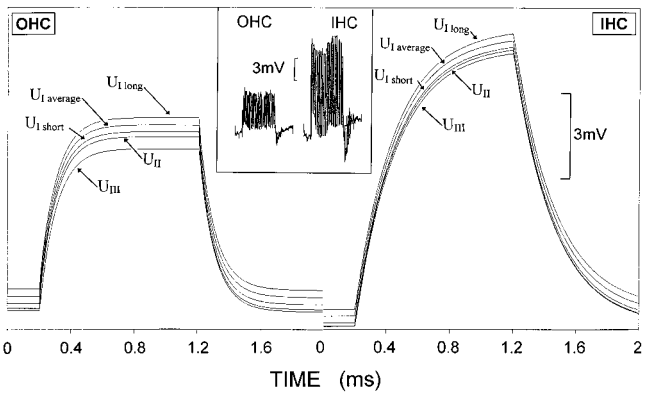

FIG. 3. Simulated receptor potentials of an inner and an outer hair cell. The voltages in the stereocilia, $U_{I\,short}$, $U_{I\,average}$ and $U_{I\,long}$, increase with lengths (OHC stereocilia lengths: 2.070 ± 1.184 μm, IHC stereocilia lengths: 2.024 ± 1.411 μm). These voltages are slightly higher than U_{II} because of the leakage through the stereocilia and compartment II. The receptor potential U_{III} is the smallest because of additional leakage through the cell body membrane. In the resting state 15% of the transduction channels are open, after 0.2 ms all transduction channels open for 1 ms. Note the following basic differences between IHC and OHC: (1) the higher gain of the IHC transduction mechanism; (2) the larger time constant of an IHC does not allow for saturation of the receptor potential within 1 ms; (3) different resting potentials, IHC: -40.9 mV and OHC: -70.4 mV. Inset (from Dallos, 1983): Receptor potentials from one inner hair cell and one outer hair cell measured in the same cochlea at a stimulation frequency of 1 kHz, 80 dB SPL. Both cells follow the stimulus simultaneously.

with the OHC value doubled. This has several reasons: Capacitance decreases when the distance between the charged particles increases, and as 70% of the OHC surface are covered with large particles of putative motor proteins (Forge, 1991) a smaller capacitance for OHC is justified. Gitter and Zenner (1990) report that IHC membrane of guinea pigs appear to be softer and less rigid than those of OHC. This makes a higher capacitance for IHC reasonable. Furthermore, a variation in membrane capacitance also occurs in generally accepted models for the membranes of the nodes of myelinated nerve fibers: Sweeney *et al.* (1987) takes for the rabbit 2.5 μF cm^{-2} as membrane capacitance and Frankenhaeuser and Huxley (1964) assume for the frog 1 μF cm^{-2}. These values are necessary for the proper shape of the action potentials.

The OHC is modeled with 900 open K^+ channels with a single channel conductance of 200 pS leading to a time constant $R_{m\,III} \cdot C_{III} = 0.1$ ms [Dallos (1984) reports a time constant of 0.127 ms]. For the IHC just 260 of those K^+ channels were assumed because of the smaller cell body area involved, this gives a time constant of 0.255 ms. Russell and Sellick (1983) report IHC time constants from 0.19 to 0.89 ms with a mean of 0.387 ms.

B. Transduction gains

The OHC is of remarkable sensitivity: In our model, a 1 ms stimulus of 12 pA (one additional open transduction channel during this time) leads to a change in receptor potential of 0.065 mV. The maximum possible range of receptor potential change is 6.6 mV. Preyer *et al.* (1994) report 5 mV.

The simulation demonstrates the higher gain to equivalent stimuli of an IHC compared to an OHC: A 1 ms stimulus of 10 pA (one additional open transduction channel during this time) leads to a receptor potential change of 0.19 mV. A receptor potential change of 0.1 mV is assumed to lead to neurotransmitter release and thereby to an action potential in the auditory nerve fiber (Hudspeth, 1989). In the case of IHC the maximum possible range of receptor potential change is 11.1 mV. This is also in accordance with experimental results (compare the inset of Fig. 3).

We have investigated the electrical influence of different stereociliary lengths on the receptor potential in order to justify a possible simplification of the model. Decreasing amplitudes of the voltages occur in the three rows of the stereocilia (U_{Ii}) in the small transition compartment (U_{II}), and in the cell body (U_{III}) (Fig. 3). Since only U_{III}, the voltage changes at the bottom of the cell, triggers neurotransmitter release, we propose the following reduction: The calculations of U_I and U_{II} can be omitted, the transduction current and some additional current, that always flows into the hair cell because of membrane leakage in the apical part (about 50 pA) are assumed to flow directly into compartment III (reduced model).

C. Transduction channel kinetics

The computer simulation allows the investigation of the influence of constant open times for all transduction channels. According to experimental results, the open times are assumed to range between 0.1 and 20 ms. Various open times at different stimulation frequencies lead to quite different results (Fig. 4). In all examples the sinusoidal stimulus is equivalent to a 20 nm amplitude, this means a 20 nm deflection of the stereocilia. For such small amplitudes the open probability of the transduction channels is a linear function of stereociliary deflection (Markin *et al.*, 1993). As we will see below, for larger displacement this function becomes asymmetric and saturating.

For this simulation each sinusoidal stimulus period is segmented in its four quadrants. The transduction channels are assumed to be stretch sensitive and therefore their opening depends not only on the deflection but also on the direction of the movement of the stereocilia: Only in the first quadrant of the stimulating signal (stereociliary motion to the lateral side) transduction channels open—and one additional channel opens for every signal step of 1 nm. The transduction channels hold their open status for a given time [0.1 ms in Fig. 4(a), 1 ms in (b) and 18 ms in (c)]. During the second quadrant of the stimulating signal, when the stereocilia move back to the initial position, the stretch on the channels is reduced again and therefore no additional channels open. In the third quadrant the stereocilia are deflected from the initial position to the medial side, some of the transduction channels that were open in the initial resting state are forced to close, for every signal step of -1 nm one channel closes. Note that in this modeling situation 20 channels are open in the initial resting state. We investigated the receptor potential reaction to a 100 Hz signal for three different transduction channel open times: 0.1, 1, and 18 ms (Fig. 4). Special effects occur when the open time of the transduction channels

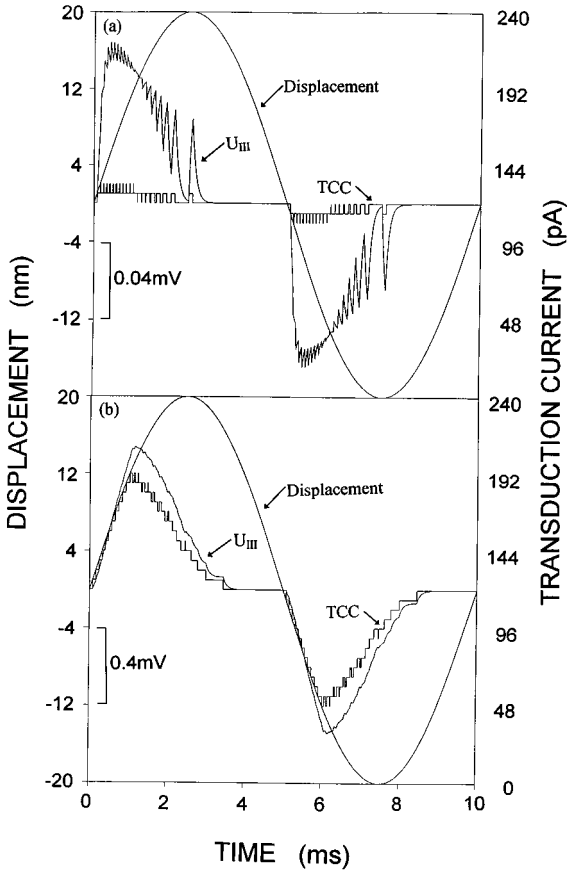

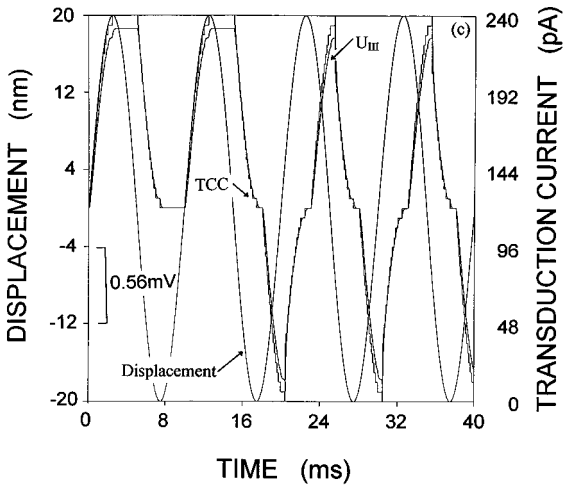

FIG. 4. Transduction channel current (TCC) and receptor potential as a function of transduction channel open time. (a) and (b) show one period, (c) shows four periods of the stimulating sinusoidal 100 Hz signal (displacement of the stereocilia) and the transduction channel current influx which rises and falls in steps of 12 pA corresponding to the single channel current. In (a) the channel open time is 0.1 ms, this is in the range of the OHC time constant $R_{m\,III} \cdot C_{III}$. Note that U_{III} accumulates more than the transduction channel current influx, but it does not reach a 0.1 mV change when two channels are open. In (b) the channel open time is 1 ms. Because of the membrane capacitance the curve for U_{III} is smoother than the steplike transduction channel current curve. Note the different voltage scale compared to (a) and that U_{III} exceeds a change of 0.1 mV. In (c) the channel open time is 18 ms and as a consequence U_{III} becomes periodical not before 18 ms. The steplike curve is the transduction channel current, because of the OHC time constant of 0.1 ms the receptor potential is nearly in phase with TCC, but smoother. Calculations with OHC parameters of Table I, reduced model.

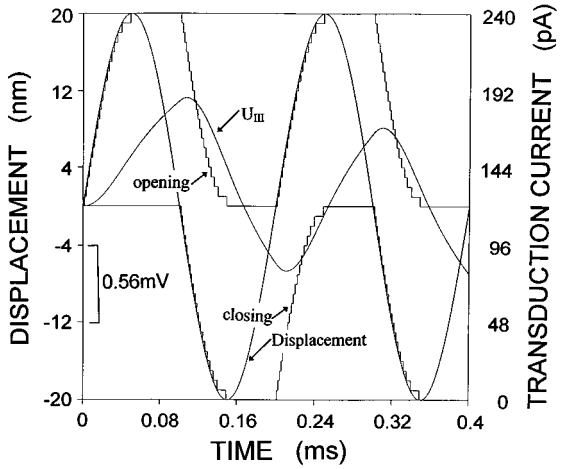

FIG. 5. Receptor potential for a 5000-Hz stimulus and a channel open time of 0.1 ms. For clarity in the TCC curve is divided into two parts: the contribution from the number of transduction channels that are open additionally to the 20 channels open at the resting state (upper step-like curve), and the contribution from the number of channels that are open at rest but closed because of stereociliary movement to the hyperpolarizing side (lower step-like curve). The sum of these two curves gives the TCC. Compared to Fig. 4(c) the phase shift of U_{III} is larger relative to the stimulating signal (OHC time constant 0.1 ms), because of its higher frequency. Calculations with OHC parameters of Table I, reduced model.

is long compared to stimulus period. Figure 4(c) demonstrates this effect for a transduction channel open time of 18 ms and stimulus period of 10 ms. During the first cycle of the stimulus, rectification of TCC and the receptor potential U_{III} occur: The transduction channel open time is 18 ms. However, during the third quadrant of the stimulating signal, other channels are forced to close. Note that compared to (a) and (b) no hyperpolarization of U_{III} occurs during the first period of the stimulus. In the second period of the stimulating signal hyperpolarization takes place, because the channels that opened during the starting phase of the stimulus close again.

For higher frequencies the transduction channel currents accumulate even for shortest open times (Fig. 5). Our results show that in the region where low frequencies are detected, longer transduction channel open times increase the amplitude of the receptor potential, whereas in high-frequency regions short transduction channel open times are of advantage because they enable hyperpolarization within a few periods of the stimulating signal.

It is known from experiments that receptor potentials in auditory hair cells are asymmetric. Markin *et al.* (1993) published an asymmetric sigmoidal relation between stereociliary displacement and the open probability of the transduction channels. This relation contributed to the results of Fig. 6 and is shown as the inset of Fig. 6(a). In (a) and (c) stimuli with an amplitude of 100 nm are used, in Fig. 6(b) the stimulus amplitude is 20 nm. Stereociliary displacements with an amplitude less than 20 nm are in a region of a linear relation to the open probability, and therefore U_{III} in Fig. 6(b) is symmetrical. Stronger stimuli lead to asymmetry in the receptor potential [Fig. 6(a) and (c)]. Stimuli in the kHz range lead because of the time constant to a steady component in U_{III} (caused by the dc component of the receptor current)

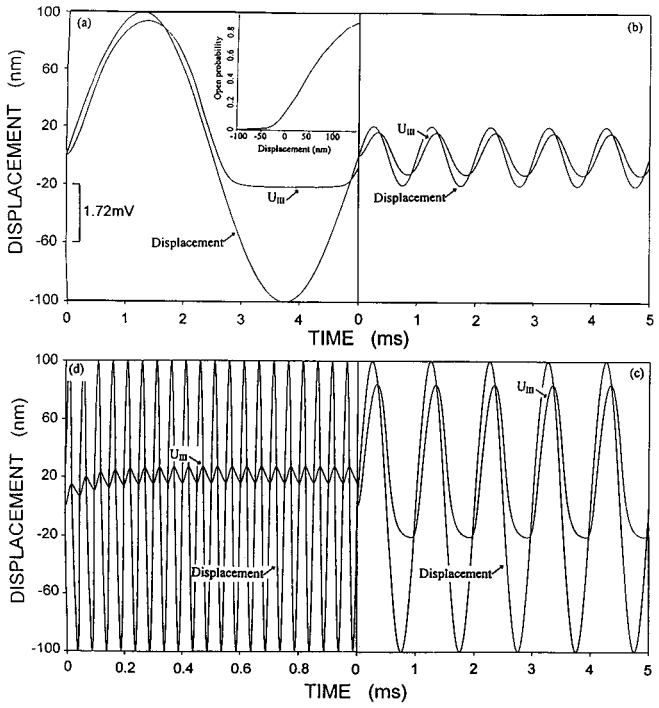

FIG. 6. Receptor potential reactions to different stimulating frequencies. Figure 6(a) shows the asymmetric receptor potential following a 200-Hz stimulus with 100-nm amplitude. The inset shows the relation between stereociliary displacement and open probability of a transduction channel according to Markin *et al.* (1993). Figure 6(b) and (c) shows the changes in U_{III} caused by 1000-Hz stimuli with amplitudes of 20 and 100 nm, respectively. In (b) U_{III} is symmetric as a consequence of the low amplitude stimulus (amplitude $<$ 20 nm), but when in (c) the high amplitude stimulus is applied, the displacement-open probability relation is not linear any more for the sinusoidal stimulus and therefore the depolarization is stronger than the hyperpolarization. In Fig. 6(d) U_{III} consists of alternating and steady components because of the high frequency stimulation: 20 kHz with 100-nm amplitude. Calculations with OHC parameters of Table I, reduced model. (a)–(d) are in the same scale regarding displacement and voltage.

which increases with frequency. The steady component in Fig. 6(d) is in the range of 1 mV, which is in accordance with experimental results from Dallos (1983) (comp. inset of Fig. 3). However, in auditory hair cells a high variance is found regarding the sensitivity and the strengths of the alternating and steady components (Mountain, 1989; Russell and Sellick, 1983; Palmer and Russell, 1986; Preyer *et al.*, 1994).

III. DISCUSSION

Taking only into account the pathway of K^+ ions through the cell and the capacitative currents results in a model that is able to represent basic properties of receptor potential changes in mammalian inner and outer hair cells. The results of our simulations are in accordance with measured receptor potentials and membrane currents, comp. the inset of Fig. 3 (from Dallos, 1983) that shows one of the rare measurements of receptor potentials for IHC and OHC from the same organ of Corti and demonstrates the higher gain of IHC. Furthermore, the asymmetric shape of the receptor potential caused by a sinusoidal stimulus [depolarizing portion is essentially larger than the hyperpolarizing one in Fig. 6(a) and (c)] was reported among others by Kros *et al.* (1993). The steady components in the receptor potential which appear at higher frequency stimulation, e.g. in Fig. 6(d), are also well known from experiments (Palmer and Russell, 1986).

Because we do not model adaptation our results reflect the behavior of hair cells with the highest sensitivity. The large dynamic range of the auditory system of $1{:}10^6$ can be explained by at least three facts: (1) for strong stimuli adaptation takes place in the hair cell; (2) the synapses of the auditory nerve fibers connecting to a single hair cell have different sensitivity; and (3) different sensitivity between neighboring hair cells.

A comparison of our results with former models shows that:

(1) Some of the former investigations did not account for the capacitance of the cell membrane because the analysis was limited to low frequencies (e.g., Mountain, 1989). Our model holds for all frequencies, calculates appropriate time constants for IHC and OHC and enables investigation of their influence on the receptor potential changes regarding different transduction channel open times and stereocilia lengths (Figs. 3, 4 and 5).
(2) Some authors use RC networks for analyzing parts of the cortical organ, but they mainly concentrate on other features than potential changes within the hair cell (e.g., Mountain and Hubbard, 1994; Dallos and Evans, 1995).
(3) A model of the receptor potential of hair cells utilizing a simple model circuit and ideas of stretch activated channels shows interesting results yet it is focused on hair cells of the lateral line organ of mudpuppy (Bell and Holmes, 1986).

Our simple electric circuit model of the mammalian auditory hair cell can be utilized to explain the following important basic features:

(1) Transduction latencies: The receptor potential follows a stimulating signal with a very short delay, i.e., with time constants of 0.1 and 0.255 ms for OHC and IHC, respectively (see Figs. 3, 5, and 6). Thus, OHC react faster. The larger IHC time constant results from an IHC membrane capacitance which is the OHC value doubled; reasons for this assumptions have been given in Sec. II. Note that these time constants (τ=RC) do not depend on the surface area since C is proportional and R is inverse proportional to the basolateral membrane area involved. The difference between IHC and OHC is, therefore, not affected by the variation in length of the OHC.
(2) Transduction gains: IHC show higher receptor potential changes to the same stimulus than OHC. This is caused by different electrical properties of both kinds of hair cells: In IHC, which are generally smaller compared to OHC of the same region, the decrease in conductance of the basolateral membrane causes higher gain.
(3) Transduction channel kinetics: In a single living hair cell the transduction channels in the stereocilia show a mixture of open times ranging from 0.1 to 20 ms. The computer simulation allows exploration of the influence of

possible channel open time distributions on the receptor potential changes. Furthermore, constant channel open times are used in order to analyze the significance of the wide range of channel open times. We have demonstrated that longer transduction channel open times cause higher gain whereas the shorter open times are of advantage for the encoding of high frequency stimuli.

In Sec. II C we used the displacement dependent open probability of the transduction channels to show the effects of different but constant open times on the receptor potential at various frequencies. A refinement of our model should investigate stochastic distributions in the transduction channel open times for the different stereocilia within one hair cell and show their effects on the receptor potential and the ability of the brain to detect the auditory signal. In that model it will be of importance to consider the fact that OHC length changes are associated with a charge movement within the cell membrane, as this charge movement manifests itself as a nonlinear membrane capacitance that contributes up to 40% of the cell's total capacitance (Santos-Sacchi, 1991).

A refinement of the model should also include the voltage dependence of the potassium channels in the basolateral cell body membrane (Gitter *et al.*, 1986; Gitter *et al.*, 1992) and the role of calcium which performs various local tasks (Jaramillo, 1995). For example, at the basal end of the hair cell depolarization-induced locally increased Ca^{++} triggers neurotransmitter release from microdomains, called active zones or ''hot spots'' (Tucker and Fettiplace, 1995).

Some interesting models deal with the macro- and micromechanical behavior of the cochlea and reproduce experimental phenomena (e.g., Furness *et al.*, 1997). Our model, which is concentrated on the electrical properties of hair cells, adequately reproduces the receptor potential changes and so is a suitable component in a multicellular model for peripheral auditory coding (Gebeshuber *et al.*, 1998).

APPENDIX: MATHEMATICAL FORMULATION OF THE MODEL

The set of equations for the voltages in the hair cell (potential earth: cortilymph potential) is the following:

$$U_{oIi}=\int \frac{I_{tc}-I_{oi}-(U_{oIi}+E_I-U_0)\cdot G_{Ii}}{C_{Ii}}dt, \tag{A1}$$

$$U_{vIi}=\int \frac{I_{st}-I_{vi}-(U_{vIi}+E_I-U_0)\cdot G_{Ii}}{C_{Ii}}dt, \tag{A2}$$

$$U_{cIi}=\int \frac{-I_{ci}-(U_{cIi}+E_I-U_0)\cdot G_{Ii}}{C_{Ii}}dt, \tag{A3}$$

$$U_{II}=\int \frac{I_{12}-I_{23}-(U_{II}+E_{II})\cdot G_{II}}{C_{II}}dt, \tag{A4}$$

$$U_{III}=\int \frac{I_{23}-(U_{III}+E_{III})\cdot (G_{III}+Kch\cdot G_K)}{C_{III}}dt, \tag{A5}$$

where U_{oIi}, U_{vIi} and U_{cIi} are the voltages in the middle of stereocilia with open transduction channels, with transduction channels changing their state from open to closed (or vice versa) and with transduction channels that are closed all the time, respectively; the index i ($i=1,2,3$) represents short, average and long stereocilia. U_{II} and U_{III} are the voltages in the middle of compartment II and the cell body, respectively. The value of the single channel current I_{tc} and other parameters taken from the literature and used for modeling are listed in Table I. I_{oi}, I_{vi} and I_{ci} represent the currents in the stereocilia, definition of the indices same as above, I_{12} is the current from the stereocilia into compartment II and I_{23} is the current from compartment II into the cell body. I_{st} denotes the stimulating transduction current in a single stereocilium, i.e. when the transduction channel is open, I_{st} equals I_{tc}, otherwise 0 pA. For the calculation of the maximum receptor potential changes, I_{st} is modeled as a current pulse with strength I_{tc} and all transduction channels are open (Fig. 3) or closed. The transduction channel open probabilities are a nonlinear and saturating function of the deflection of the stereocilia [inset Fig. 6(a)] and determine the time course of I_{st} for each stereocilium (Figs. 4, 5, and 6; the sum of the currents I_{st} through all stereocilia gives the whole cell transduction channel current TCC).

The membrane conductivities and capacities in Eqs. (A1)–(A5) are

$$C_{Ii}=a_{Ii}\cdot c, \quad G_{Ii}=a_{Ii}\cdot gm, \quad \text{with } a_{Ii}=d_I\cdot\pi\cdot l_{Ii}+d_I^2\cdot\frac{\pi}{4}, \tag{A6}$$

$$C_{II}=a_{II}\cdot c, \quad G_{II}=a_{II}\cdot gm, \quad \text{with } a_{II}=d_{II}^2\cdot\frac{\pi}{4}-n\cdot d_I^2\frac{\pi}{4}, \tag{A7}$$

$$C_{III}=a_{III}\cdot c, \quad G_{III}=a_{III}\cdot gm, \quad \text{with } a_{III}=d_{III}\cdot\pi\cdot l_{III}+d_{III}^2\cdot\frac{\pi}{4}, \tag{A8}$$

where a denotes area, d diameter and l length: $d_I=0.2$ μm, $d_{II}=d_{III}=10$ μm, $l_{I1}=0.886$ μm (short), $l_{I2}=2.07$ μm (average), $l_{I3}=3.254$ μm (long), $l_{II}=1$ μm, $l_{III}=50$ μm.

The currents in the hair cell are calculated as follows:

$$I_{oi}=\frac{U_{oIi}-U_{II}}{\frac{R_{Ii}}{2}+\frac{R_{II}}{2}}, \quad I_{vi}=\frac{U_{vIi}-U_{II}}{\frac{R_{Ii}}{2}+\frac{R_{II}}{2}}, \quad I_{ci}=\frac{U_{cIi}-U_{II}}{\frac{R_{Ii}}{2}+\frac{R_{II}}{2}}, \tag{A9}$$

$$I_{I2i}=I_{oi}\cdot m_{oi}+I_{vi}\cdot m_{aoi}+I_{ci}\cdot(n_i-m_{oi}-m_{aoi}), \tag{A10}$$

$$I_{I2}=I_{I21}+I_{I22}+I_{I23}, \quad I_{23}=\frac{U_2-U_3}{R_2/2+R_3/2}. \tag{A11}$$

The cytoplasm resistances in Eq. (A9) are

$$R_{Ii}=\frac{\rho_i\cdot l_{Ii}}{0.25\pi\cdot d_1^2}, \quad R_{II}=\frac{\rho_i\cdot l_{II}}{0.25\pi\cdot d_{II}^2}, \quad R_{III}=\frac{\rho_i\cdot l_{III}}{0.25\pi\cdot d_{III}^2},$$

m_o is the number of open transduction channels, m_{ao} is the number of transduction channels additionally open to the 15% open at rest [m_{ao} ranges from -15 (i.e., all TC closed) to $+85$ (i.e., all TC open) for OHC, and from -9 to $+51$ for IHC] and n_i denotes the number of stereocilia in each row.

Bell, J., and Holmes, M. H. (**1986**). ''A nonlinear model for transduction in hair cells,'' Hearing Res. **21**, 97–108.

Cody, A. R., and Russell, I. J. (**1987**). ''The responses of hair cells in the basal turn of the guinea-pig cochlea to tones,'' J. Physiol. (London) **383**, 551–569.

Crawford, A. C., Evans, M. G., and Fettiplace, R. (**1991**). ''The actions of calcium on the mechanoelectrical transducer current of turtle hair cells,'' J. Physiol. (London) **434**, 369–398.

Dallos, P. (**1983**). ''Cochlear electroanatomy: influence on information processing,'' in: *Hearing—Physiological Bases and Psychophysics*, edited by R. Klinke and R. Hartmann, Proc. 6th Int. Symp. on Hearing (Springer, Berlin), pp. 32–38.

Dallos, P. (**1984**). ''Some electrical circuit properties of the organ of Corti. II. Analysis including reactive elements,'' Hearing Res. **14**, 281–291.

Dallos, P., and Evans, B. N. (**1995**). ''High-frequency motility of outer hair cells and the cochlear amplifier,'' Science **267**, 2006–2009.

Dallos, P., and Santos-Sacchi, J. (**1982**). ''Intracellular recordings from cochlear outer hair cells,'' Science **218**, 582–584.

Forge, A. (**1991**). ''Structural features of the lateral walls in mammalian cochlear outer hair-cells,'' Cell Tissue Res. **265**, 473–483.

Frankenhaeuser, B., and Huxley, A. L. (**1964**). ''The action potential in the myelinated nerve fibre of Xenopus Laevis as computed on the basis of voltage clamp data,'' J. Physiol. (London) **171**, 302–315.

Furness, D. N., Zetes, D. N., Hackney, C. M., and Steele, C. R. (**1997**). ''Kinematic analysis of shear displacement as a means for operating mechanotransduction channels in the contact region between adjacent stereocilia of mammalian cochlear hair cells,'' Proc. R. Soc. London, Ser. B **264**, 45–51.

Gebeshuber, I. C., Mladenka, A., Rattay, F., and Svrcek-Seiler, W. A. (**1998**). ''Brownian motion and the ability to detect weak auditory signals,'' in *Chaos and Noise in Biology and Medicine* edited by C. Taddei-Ferretti (World Scientific, Singapore, in press).

Gitter, A. H. (**1994**). ''Sind 'tip links' Grundlage der Mechanosensitivität von Haarzellen?'' HNO **42**, 327–333.

Gitter, A. H. (**1996**). ''Row-to-row horizontal links may be associated with the transduction channels of hair cells,'' ORL **58**, 1–3.

Gitter, A. H., Frömter, E., and Zenner, H. P. (**1992**). ''C-type potassium channels in the lateral cell membrane of guinea-pig outer hair cells,'' Hearing Res. **60**, 13–19.

Gitter, A. H., Zenner, H. P., and Frömter, E. (**1986**). ''Membrane potential and ion channels in isolated outer hair cells of guinea pig cochlea,'' ORL J. Otorhinolaryngol. Relat. Spec. **48**, 68–75.

Gitter, A. H., and Zenner, H. P. (**1990**). ''The cell potentials of isolated inner hair cells *in vitro*,'' Hearing Res. **45**, 87–94.

Hudspeth, A. J. (**1989**). ''How the ear's works work,'' Nature (London) **341**, 397–404.

Hudspeth, A. J., and Corey, D. P. (**1977**). ''Sensitivity, polarity, and conductance change in the response of vertebrate hair cells to controlled mechanical stimuli,'' Proc. Natl. Acad. Sci. USA **74**, 2407–2411.

Jaramillo, F. (**1995**). ''Signal transduction in hair cells and its regulation by calcium,'' Neuron **15**, 1227–1230.

Katz, B., and Miledi, R. (**1967**). ''A study of synaptic transmission in the absence of nerve impulses,'' J. Physiol. (London) **192**, 407–436.

Konishi, T., and Salt, A. N. (**1983**). ''Electrochemical profile for potassium ions across the cochlear hair cell membranes of normal and noise-exposed guinea pigs,'' Hearing Res. **11**, 219–233.

Kros, C. J., Rüsch, A., Lennan, G. W. T., and Richardson, G. P. (**1993**). ''Voltage dependence of transducer currents in outer hair cells of neonatal mice,'' in *Biophysics of Hair Cell Sensory Sytems* edited by H. Duifhuis, J. W. Horst, P. van Dijk, and S. M. van Netten (World Scientific, Singapore), pp. 141–150.

Ma, Y. L., Rarey, K. E., Gerhardt, K. J., Curtis, L. M., and Rybak, L. P. (**1996**). ''Electrochemical potentials and potassium concentration profiles recorded from perilymph, endolymph and associated inner ear tissues in adrenalectomized rats,'' Hearing Res. **96**, 151–156.

Markin, V. S., Jaramillo, F., and Hudspeth, A. J. (**1993**). ''The three-state model for transduction-channel gating in hair cells,'' Biophys. J. **64**, A93.

Mountain, D. C. (**1989**). ''Measurement of low-frequency receptor potentials in inner hair cells: a theoretical analysis,'' Hearing Res. **41**, 101–106.

Mountain, D. C., and Hubbard, A. E. (**1994**). ''A piezoelectric model of outer hair cell-function,'' J. Acoust. Soc. Am. **95**, 350–354.

Palmer, A. R., and Russell, I. J. (**1986**). ''Phase-locking in the cochlea nerve of the guinea-pig and its relation to the receptor potential of inner hair cells,'' Hearing Res. **24**, 1–15.

Pickles, J. O., Comis, S. D., and Osborne, M. P. (**1984**). ''Cross-links between the stereocilia in the guinea pig organ of Corti, and their possible relation to sensory transduction,'' Hearing Res. **15**, 103–112.

Preyer, S., Hemmert, W., Pfister, M., Zenner, H. P., and Gummer, A. W. (**1994**). ''Frequency response of mature guinea-pig outer hair cells to stereociliary displacement,'' Hearing Res. **77**, 116–124.

Rattay, F. (**1990**). *Electrical Nerve Stimulation: Theory, Experiments and Applications* (Springer Wien/New York).

Russell, I. J., and Sellick, P. M. (**1978**). ''Intracellular studies of hair cells in the mammalian cochlea,'' J. Physiol. (London) **284**, 261–290.

Russell, I. J., and Sellick, P. M. (**1983**). ''Low-frequency characteristics of intracellularly recorded receptor potentials in guinea-pig cochlear hair cells,'' J. Physiol. (London) **338**, 179–206.

Santos-Sacchi, J. (**1991**). ''Reversible inhibition of voltage-dependent outer hair-cell motility and capacitance,'' J. Neurosci. **11**, 3096–3110.

Spoendlin, H. (**1970**). ''Vestibular labyrinth,'' in *Ultrastructure of the Peripheral Nervous System and Sense Organs*, edited by A. Bischoff (Georg Thieme Verlag, Stuttgart), p. 264.

Sweeney, J. D., Mortimer, J. T., and Durand, D. (**1987**). ''Modeling of mammalian myelinated nerve for functional neuromuscular electrostimulation,'' IEEE 9th Annual Conference Eng. Med. Biol. Soc. Boston, 1577–1578.

Tucker, T., and Fettiplace, R. (**1995**). ''Confocal imaging of calcium microdomains and calcium extrusion in turtle hair cells,'' Neuron **15**, 1323–1335.

Zenner, H. P. (**1994**). ''Physiologische und biochemische Grundlagen des normalen und gestörten Gehörs,'' in *Oto-Rhino-Laryngologie in Klinik und Praxis*, edited by J. Helms (Georg Thieme Verlag, Stuttgart), Vol. 1: Ohr, pp. 81–230.

Zetes, D. E. (**1995**). ''Mechanical and morphological study of the stereocilia bundle in the mammalian auditory system.'' Ph.D. Thesis, Stanford University.